Fiber alignment angles effect on the tensile performance of laminated bamboo lumber

Dong Yang[1a,1b], Haitao Li[1a,1b*], Zhenhua Xiong[2], Rodolfo Lorenzo[3], Ileana Corbi[4], Ottavia Corbi[4]

[1a] College of Civil Engineering, Nanjing Forestry University, Nanjing 210037, China; [1b] Joint International Research Laboratory of Bio-composite Building Materials and Structures, Nanjing Forestry University, Nanjing 210037, China

[2] Ganzhou Sentai bamboo company LTD, Ganzhou 341001, China.

[3] University College London, London WC1E 6BT, UK.

[4] University of Naples Federico II, Via Claudio 21,80133 Naples, Italy.

*Corresponding author: Haitao LI, Professor, E-mail: lhaitao1982@126.com

Abstract: For better application of laminated bamboo lumber (LBL) in construction industry, the tensile performance of LBL was studied by conducting tension test on LBL specimens with seven different fiber alignment angles, each alignment angle containing 30 specimens. All the specimens only experienced the elastic stage before brittle failure with four failure types. With increasing alignment angle, the tensile strength, tensile modulus, and ultimate tension strain decreased rapidly from 0° to 30°, while they almost remained constants after the angle of 45°. Hankinson's formula (n=1.75) can be used to predict the tensile strength of LBL. An empirical equation was proposed to predict the tensile modulus of LBL. The Poisson's ratio increased and peaked at 15° before declining. Based on the stress-strain coordinate transformation, the relation between shear properties and the alignment angle of LBL was studied; the calculated shear strength decreased with increasing alignment angle, and an empirical equation was proposed which could be used to obtain the shear strength of LBL for engineering use.

Key words: laminated bamboo lumber, off-axis tension test, mechanical properties, fiber alignment angle

1 Introduction

Due to the constant growth of urbanized areas, the carbon emissions associated with the construction industry has raised causing global warming acceleration. Two of the common conventional materials used in construction industry, steel and concrete (Corbi et al. 2021), are responsible for 44% of industrial carbon dioxide emissions globally (Allwood et al. 2012). Bamboo, a low-carbon emission material which gains more and more attention, has potential as alternative construction material to balance high building demand with a positive environmental impact. (Ghavami 2008; Li et al. 2021; Lou et al. 2021; Yuan et al. 2021)

Similar to wood (Bi et al. 2021), natural bamboo pole has been used as a construction material for a long time (Li and Lou 2021; Liu et al. 2021; Xiao et al. 2021) . However, it is easily to decay in less than 24 months in natural environment due to fungi and insects (Chen et al. 2007; Sun et al. 2017), also, uneven shrinkage (Wu 1992) could also happen because of the change of temperature between seasons. Furthermore, the organic geometry, physical and mechanical properties of natural bamboo are very different (Lorenzo et al. 2020a, 2020b; Lei et al. 2021), making natural bamboo pole cannot meet the requirement of modern structure. The appearance of engineered bamboo (Liu et al. 2020a; Xiao et al. 2013; Zhong et al. 2017; Wei et al. 2020; Huang et al. 2015; Liu et al. 2020b) relieves most of the shortcomings of natural bamboo, this paper studies laminated bamboo lumber (Su et al. 2021).

LBL is an anisotropic material and could be simplified as orthotropic material (Takeuchi et al. 2016) with excellent mechanical properties. Test results from Sharma et al (2017) proved that the compressive strength, tensile strength, shear strength, and stiffness were comparable to that of wood products. Correal et al. (2014) conducted a comprehensive study on the physical and mechanical properties of LBL and concluded that glued laminated Guadua bamboo possessed equivalent strength and stiffness to commonly

used engineered wood in the United States, showing its great potential in light frame structure. Mahdavi et al. (2011) reviewed and summarized the production technology, mechanical properties, and economic benefits of LBL, and considered that LBL can be applied in modern structure. Through a large number of experiments, Li et al. (2013, 2015b) analyzed the failure modes and proposed a constitutive model of LBL. To investigate the effect of layered structure of LBL on the mechanical performance, Lee et al. (2012) studied five different layered structure types and found out that the cross-layered type was better than others. To better promote the use of LBL in the construction industry (Zhou et al. 2021; Ponzo et al. 2021), many scholars have further studied the mechanical properties of laminated bamboo components, such as beams (Sinha et al. 2014; Díaz et al. 2013; Xu et al. 2018), columns (Li et al. 2015a), and connections (Khoshbakht et al. 2018; Leng et al. 2020; Chen et al. 2020).

At present, there are many studies on the mechanical properties of LBL (Dauletbek et al. 2021; Verma and Chariar 2013), but the research on the off-axis mechanical properties is still little. In a real structure, the load direction could be varied. Moreover, LBL is an orthotropic material rather than a homogeneous material, thus it is more important to study the influence of different load directions. Previous work has been done on the off-axis compression performance of LBL (Yang et al. 2020). Chow et al. (2019) also studied the tensile strength and tensile modulus of LBL and three failure criteria were used to fit the test results. To make up for the lack of existing research, this paper studied the off-axis tensile properties of LBL based on the test of 210 specimens with seven different alignment angles, summarized the changes of tensile modulus, tensile strength and Poisson's ratio with the change of alignment angles, put forward the tensile stress-strain model, and studied the applicability of empirical formulas to LBL. In addition, the test method of shear strength and shear modulus for LBL was studied based on the stress and strain coordinate

transformation.

2 Test design

2.1 Manufacturing process of LBL

The raw material (*Phyllostachys pubescens*) was from Yong'an, Fujian Province, China. Natural bamboo poles were split and peeled into bamboo strips as basic units with the size of 2005mm×21mm×7mm. After being glued with resorcinol as adhesive and arranged, LBL were made by pressing bamboo strips at 157℃ for around fifteen minutes with main pressure of 9 MPa, side pressure of 6.5 MPa. The density of LBL was 689kg/m^3. All the specimens were from Ganzhou Sentai Bamboo Co., Ltd.

2.2 Specimens

The size of the specimens was designed with reference to ASTM D143 (ASTM International 2014). According to the different fiber directions and loading directions caused by different alignment angles, the test specimens were divided into 7 groups with angles of 0°, 15°, 30°, 45°, 60°, 75° ,90°. The number of specimens in each group was 30, and the naming rule of each group was "T + alignment angle". The production process and dimensions of the test piece are shown in Fig.1.

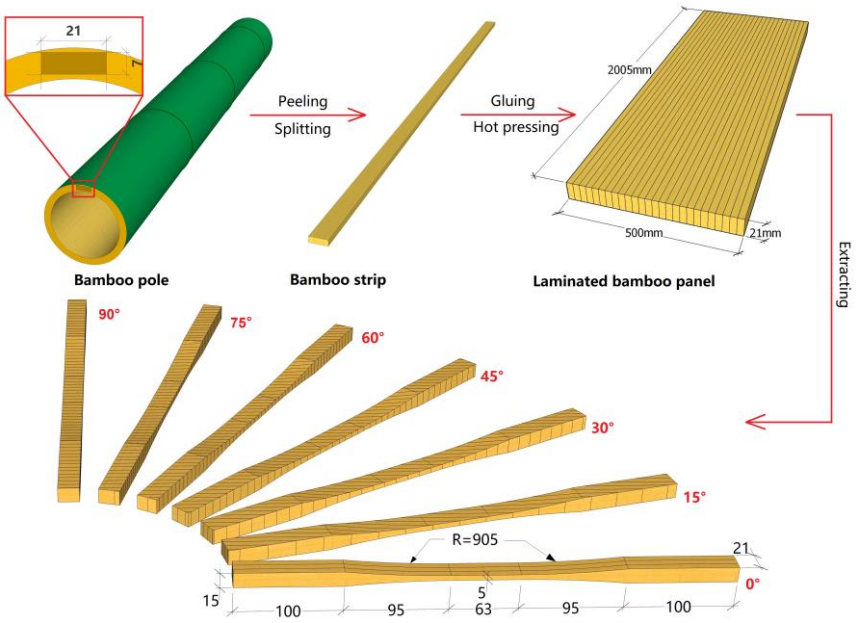

Fig.1 Manufacturing process and dimension of LBL specimens

2.3 Test method

All tests were conducted by using a universal testing machine with maximum load of 50kN, and all test data was collected by a static data acquisition instrument TDS-530 manufactured by Tokyo Measuring Instruments Laboratory Co., Ltd., Tokyo, Japan. The manufacturer of the strain gauges was Huangyan Linli Engineering Sensor Factory, Zhejiang, China. Three strain gauges were attached on each side in the middle of the specimen to collect the vertical, transverse and 45° oblique strains with cyanoacrylate as adhesive from Taizhou Henco-glue Co., Ltd, Zhejiang, China. The angle between each two adjacent strain gauges was 45°. Load control was adopted, and all tests were completed after about 5 minutes. The test design and method of attaching the strain gauges are shown in Fig.2.

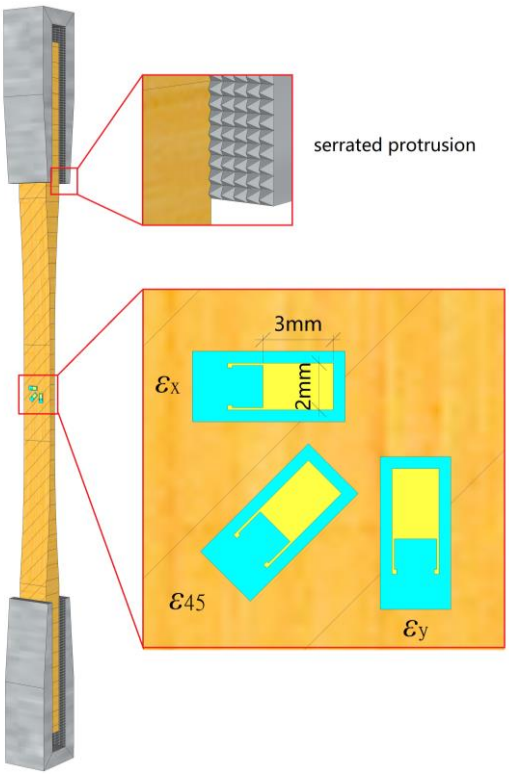

Fig.2 Test design and strain gauges attachment method

3 Failure phenomena

All the specimens showed brittle failure. Four failure types were classified according to the alignment angles of LBL as shown in Fig.3.

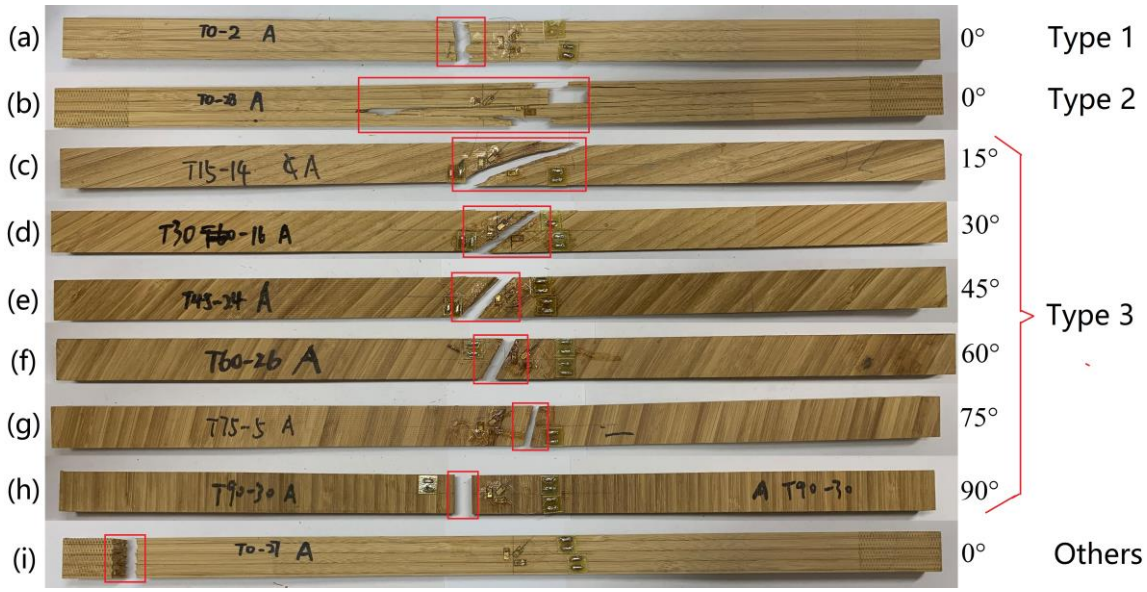

Fig.3 Typical failure types for specimens with different fiber alignment angles

3.1 Specimens of group T0

Failure type 1 was due to fiber tension breakage. During the loading process, the load of bamboo fiber increased rapidly until the ultimate bearing capacity was reached with sudden breakage of all bamboo fibers, showing brittle failure (Fig.3a). Failure type 1 was an ideal failure mode. However, due to the variability of organic mechanical properties of raw bamboo such as position of bamboo nodes, only three specimens were in type 1, while more specimens showed type 2 failure.

Failure type 2 was also fiber breakage failure while it was different from failure type 1. Each specimen in T0 group was composed of three bamboo strips with organic mechanical difference. Although the difference was not significant, it still led to one of the three bamboo strips snapping first, causing a certain eccentric tension which resulted in the specimen tearing between the laminate layers, as shown in Fig.3(b).

3.2 Specimens of all other groups

Specimens with an angle from 15° to 90° showed transverse tearing between fibers. When the ultimate load was reached, the bonding part between bamboo fibers cannot bear greater force, which was failure type 3, as shown in Fig.3(c-h).

3.3 Others

The above failure modes were all strength failure. However there were still specimens were damaged because of the stress concentration at the clamping end, which was type 4, as shown in Fig.3(i). This was not an expected failure type, but it was still recorded for data integrity, including 1 specimen in group T0, 2 in T45, 1 in T60 and 5 in T90.

4 Test results and analysis

4.1 Calculations of test results

The tensile strength of LBL was calculated by Eq.(1):

$$f_{t,\theta} = P_{t,u} / A \tag{1}$$

where, $f_{t,\theta}$ is the tensile strength of specimen with the alignment angle θ; $P_{t,u}$ is the ultimate load; A is the sectional area of the middle part of the specimen.

The tensile modulus was calculated by Eq.(2):

$$E_{t,\theta} = \Delta\sigma_x / \Delta\varepsilon_x = \Delta P_t / \left(A\Delta\varepsilon_x\right) \tag{2}$$

where, $E_{t,\theta}$ is the tensile modulus of specimen with the alignment angle θ; ΔP_t is the load increment; $\Delta\varepsilon_x$ is the strain increment in the loading direction.

The Poisson's ratio was calculated by Eq.(3):

$$\mu_\theta = \left|\Delta\varepsilon_y\right| / \left|\Delta\varepsilon_x\right| \tag{3}$$

where, μ_θ is Poisson's ratio of specimen with the angle θ; $\Delta\varepsilon_x$, $\Delta\varepsilon_y$ are the strain increment parallel and perpendicular to the loading direction.

The calculated test results and tensile properties of LBL were compared with wood and wood-based products, as shown in Table 1. Since failure type 4 was not an ideal type, thus the data in Table 4 does not include specimens with failure type 4.

Table 1 Test results

Group		Ultimate load/N	Tensile Strength/MPa	Tensile modulus/MPa	Ultimate strain	Poisson's ratio
T0	Mean	14007	128.2	11294	0.013	0.268
	COV	0.111	0.109	0.050	0.155	0.148
	CHV	11404	105.0	10343	0.0093	-
T15	Mean	2512.7	52.10	7720.8	0.0078	0.298
	COV	0.212	0.219	0.143	0.339	0.275
	CHV	482.50	33.10	5879.1	0.0033	-
T30	Mean	1416.3	24.00	4077.0	0.0069	0.265
	COV	0.307	0.307	0.174	0.385	0.251
	CHV	40.400	11.60	2889.5	0.0024	-

T45	Mean	1328.9	15.00	2303.3	0.0077	0.207
	COV	0.152	0.156	0.153	0.400	0.448
	CHV	966.50	11.20	1715.5	0.0025	-
T60	Mean	1351.7	12.20	2438.5	0.0053	0.155
	COV	0.096	0.081	0.133	0.178	0.257
	CHV	1134.6	10.50	1897.3	0.0038	-
T75	Mean	965.70	9.100	1640.7	0.0065	0.102
	COV	0.192	0.164	0.248	0.337	0.377
	CHV	656.80	6.600	961.00	0.0028	-
T90	Mean	795.00	8.100	2371.3	0.0035	0.0790
	COV	0.185	0.179	0.149	0.207	0.222
	CHV	549.00	5.800	1782.1	0.0023	-

Note: COV is coefficient of variation; CHV is characteristic value, CHV = mean value * (1 - v × COV), v is determined by the number of samples (British Standard 2002)

4.2 Load-displacement curves

Load-displacement curves of all groups are shown in Fig.4(a-g). Typical load-displacement curves of each group are shown in Fig.4(h). The load displacement curves of each group of specimens are approximately a straight line, except for the specimen with 0°. This is because the clamping force of the loading head gradually increased with increasing tensile force, and then the serrated protrusion on the clamp caused ‘bite marks’ on the specimen, resulting in a slight slip. With the increase in displacement, the load increased linearly, and when the ultimate load was reached, the load dropped suddenly. The selected load-displacement curves from different groups of specimens are shown in Fig.4(h). The numbers after “-“ were the number of specimens. It is vividly that the ultimate load and displacement also decreased with the increase in the alignment angle.

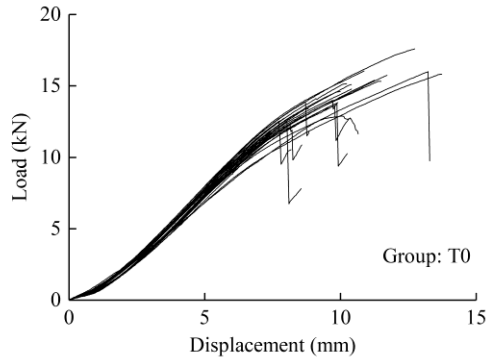
Load (kN)
Displacement (mm)
Group: T0

(a)

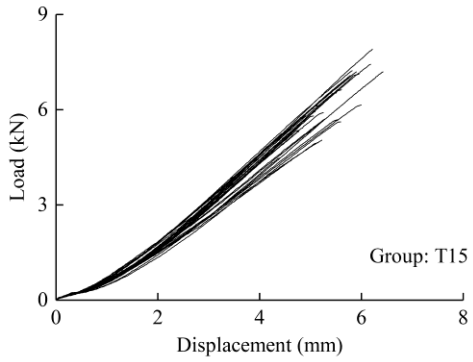
Load (kN)
Displacement (mm)
Group: T15

(b)

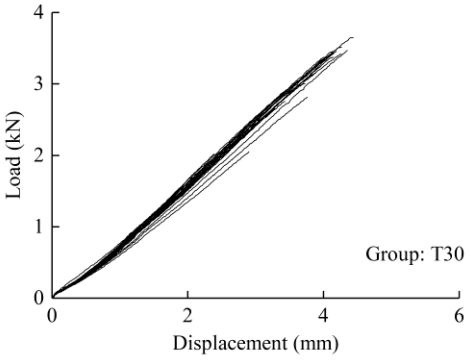
Load (kN)
Displacement (mm)
Group: T30

(c)

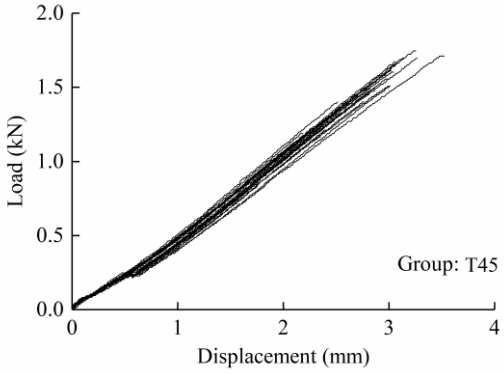
Load (kN)
Displacement (mm)
Group: T45

(d)

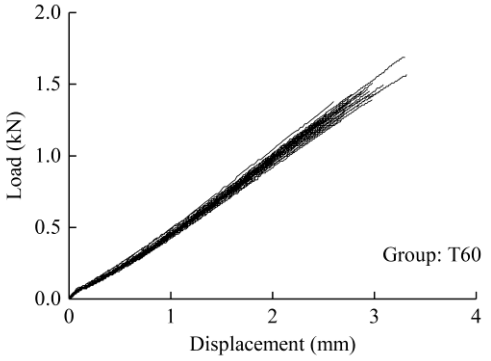
Load (kN)
Displacement (mm)
Group: T60

(e)

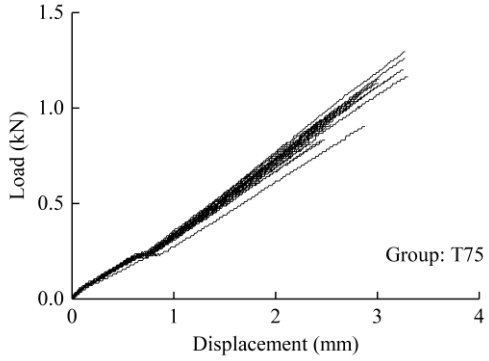
Load (kN)
Displacement (mm)
Group: T75

(f)

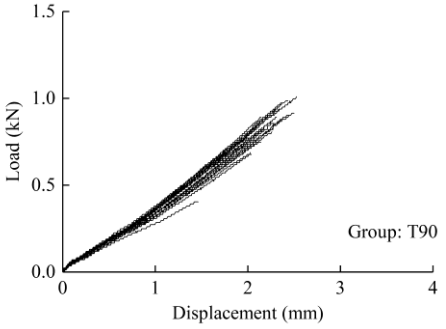
Load (kN)
Displacement (mm)
Group: T90

(g)

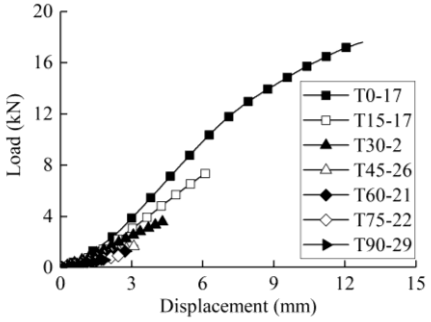
Load (kN)
Displacement (mm)
T0-17
T15-17
T30-2
T45-26
T60-21
T75-22
T90-29

(h)

Fig.4 Typical load-displacement curves

4.3 Stress-strain curves

Stress-strain curves and model values calculated by Eq.(4) of each group of specimens are shown in the Fig.5(a-g), and typical stress-strain curves of each group are shown in the Fig.5(h). Similar to the load displacement relation, the stress-strain relation was linear. Therefore, the tensile stress-strain relation of LBL at various alignment angles can be expressed by Eq.(4). When the alignment angle was between 0° and 30°, the tensile modulus, which is the slope of each curve, decreased significantly. While when the alignment angle was greater than or equal to 45°, the tensile modulus started to be stable. The ultimate strength and ultimate strain of each group of specimens showed the same rule.

$$\sigma_{t,\theta} = E_{t,\theta}\varepsilon \tag{4}$$

where, $\sigma_{t,\theta}$, ε, and $E_{t,\theta}$ are the corresponding tensile stress, tensile strain, and elastic modulus of specimens with the angle θ, respectively.

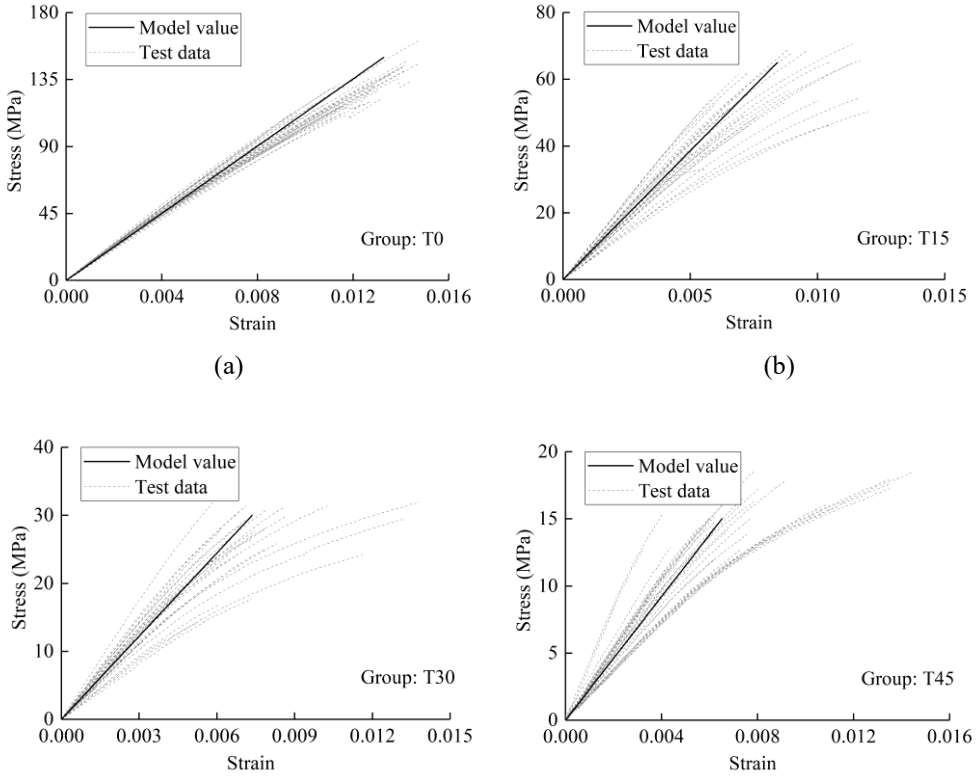

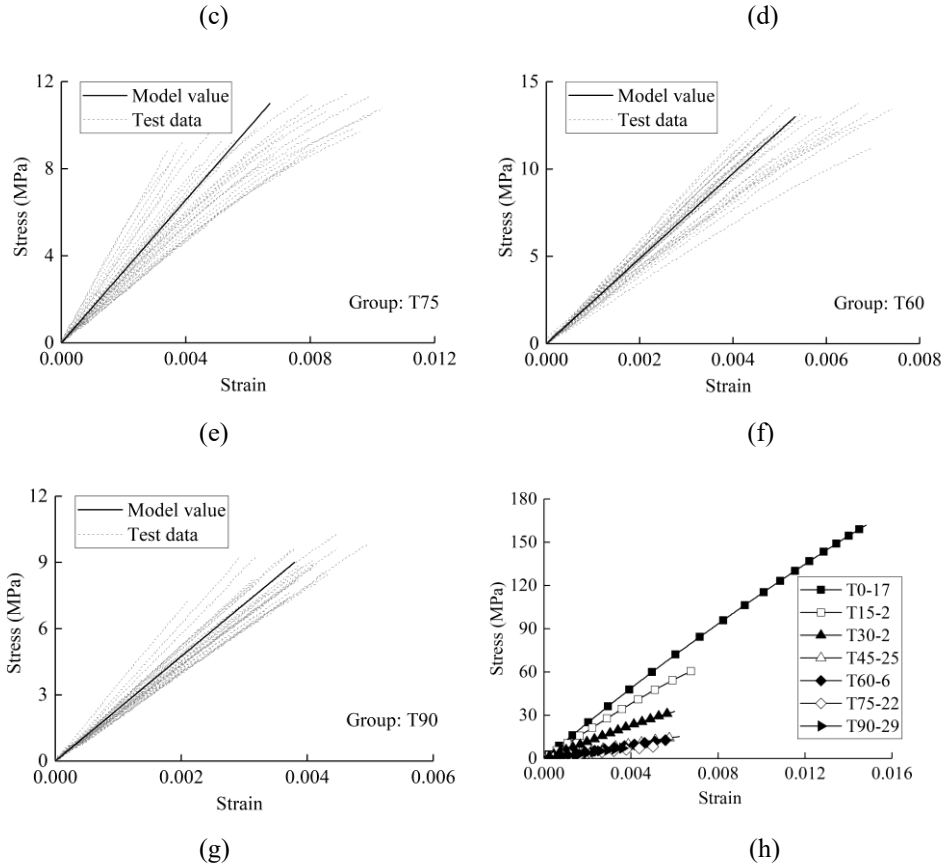

Fig.5 Typical stress-strain curves

4.4 Analysis of tensile strength

At present, there is much research on the tensile strength of wood with different angles. Some empirical formulas ignoring the shear effect have been put forward, and classical failure criteria have also been applied.

In Chinese code GB 50005 (National Standards of China 2003), the equation for calculating the off-axis tensile strength of wood is an empirical formula:

$$f_{t,\theta} = f_1 / \left[1+\left(f_1 / f_2 - 1\right)\left(\theta - 10^{o}\right)\sin\theta / 80^{o}\right] \tag{5}$$

where, $f_{t,\theta}$ is the tensile strength when the alignment angle is θ; f_1, f_2 are the tensile strength of LBL parallel and perpendicular to the grain, respectively.

Hankinson (1921) proposed an empirical formula based on off-axis compression test of timber:

$$f_{t,\theta} = f_1 f_2 / \left(f_1 \sin^2 \theta + f_2 \cos^2 \theta \right) \tag{6}$$

Bodig and Jayne (1982) developed Hankinson formula, rewriting Hankinson formula into:

$$f_{t,\theta} = f_1 f_2 / \left(f_1 \sin^n \theta + f_2 \cos^n \theta \right) \tag{7}$$

where, n is a constant. Different values of n were t in this paper.

According to the test results, the tensile strength of LBL from 0° to 90° was generally in a downward trend, especially significant from 0° to 30°. While when the angle is greater than 45°, the tensile strength was almost a constant. The tensile strength perpendicular to grain (90°) of LBL was about one sixteenth of the tensile strength parallel to grain (0°), and the strength of 15° was only less than half of the 0° specimen. Therefore, the tensile situation perpendicular to grain should be avoided in engineering application.

Figure 6 shows a comparison of the predicted curves of tensile strength obtained by GB 50005 and revised Hankinson's formula. The predicted results of GB 50005 and Hankinson's formula with n = 2 and 2.5 were larger than the test results when θ < 45°, while the prediction result with n = 1.5 was smaller. Hankinson's formula with n=1.75 was more reasonable to predict tensile strength of LBL from Fig.6.

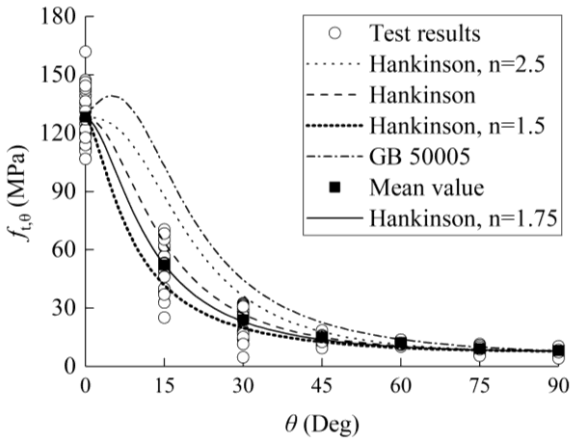

Fig.6 Prediction of tensile strength

4.5 Tensile modulus

As mentioned above, the tensile modulus of LBL gradually decreased with increasing alignment angle.

The tensile modulus decreased rapidly from 0° to 30°. However, when the angle was greater than 45°, the tensile modulus could be regarded as a constant. In this paper, the tensile modulus of LBL predicted by some empirical formulas was studied.

The Hankinson's formula developed by Bodig and Jayne (1982) can also be used to predict the tensile modulus of materials:

$$E_{t,\theta} = E_1 E_2 / \left(E_1 \sin^n \theta + E_2 \cos^n \theta \right) \tag{8}$$

where, E_1, E_2 are the elastic modulus of the LBL with the angle 0° and 90°, respectively.

Different values of n (n = 1.25, 1.5, 2) were taken into Eq.(8), as shown in Fig.8. The curves were not consistent with the test results, thus we proposed an empirical equation:

$$\frac{1}{E_{t,\theta}} = \frac{\cos^4 \theta}{E_1} + \frac{\sin^4 \theta}{E_2} + \frac{\alpha \cos^2 \theta \sin^2 \theta}{E_1} \tag{9}$$

where, α is a constant and its value is 10.

Prediction of tensile modulus of each formula is shown in Fig.7. The predicted curve of Eq.(9) is more reasonable than Hankinson's formula.

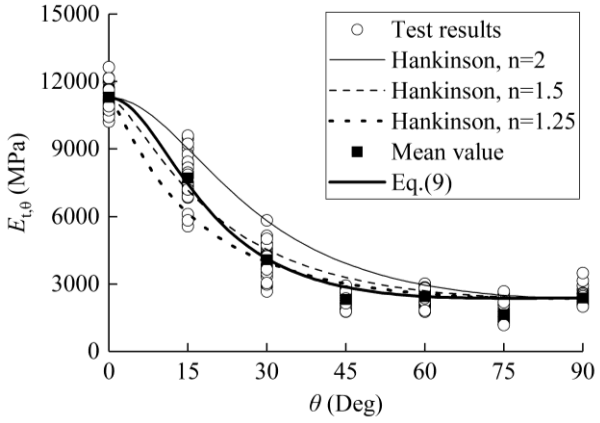

Fig.7 Prediction of tensile modulus

4.6 Ultimate strain

All the LBL tension specimens were destroyed immediately when the ultimate load or ultimate strain

were reached, showing brittle failure. Although the tensile strength of the LBL was relatively high compared with wood, the ultimate strain was still small, which has a great influence on the practical engineering application. In this section, the ultimate tensile strain of LBL was studied.

Figure 8 shows the relation between alignment angle and ultimate strain, which was measured from strain gauge ε_{45} in Fig.2. The mean value of ultimate strain showed a downward trend from 0° to 15°, while the decreasing trend was not significant from 30° to 90°. The characteristic value (CHV) with 95% guarantee rate of ultimate strain also showed a similar trend. The recommended strain value for engineering design could be given according to the characteristic value, which is 0.0093 for specimens with 0° alignment angle, while 0.0023 for other angles. The ultimate tensile strain can be approximately fitted by a cubic curve with R^2=0.6440:

$$\varepsilon_{u,\theta} = 0.012 - 3.530\times10^{-4}\theta + 7.251\times10^{-6}\theta^2 - 4.887\times10^{-8}\theta^3 \quad (10)$$

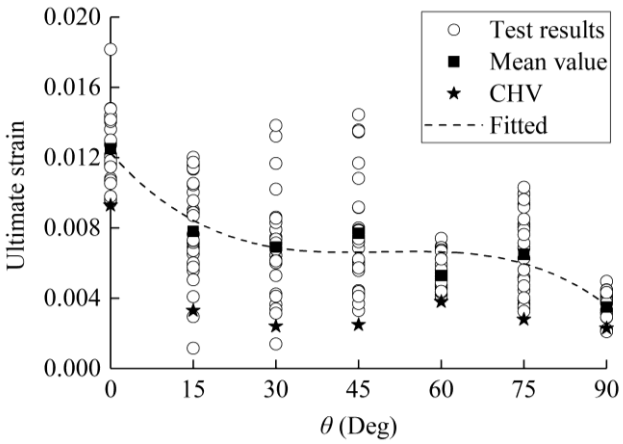

Fig.8 Ultimate strain

4.7 Poisson's ratio

Figure 9 shows the Poisson's ratio, which increased first from 0° to 15° and then declined gradually from 15° to 90° degrees. This is similar to the results from Pindera and Herakovich (1986) for graphite/polyimide unidirectional composites. The mean value of Poisson's ratio can be expressed by a cubic function with

R^2=0.6388:

$$\mu_\theta = 0.270 + 0.003\theta - 1.496\times10^{-4}\theta^2 + 9.696\times10^{-7}\theta^3 \tag{11}$$

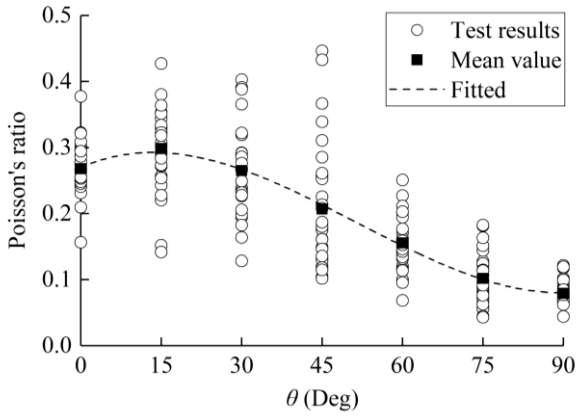

Fig.9 Poisson's ratio

5 Evaluation of shear properties for engineering use

According to the strain and stress coordinate transformation, the shear modulus (G) and shear strength (S) of LBL could be obtained by off-axis tension test:

$$G = \frac{-P_t \sin\theta\cos\theta / A}{2\left(\varepsilon_y - \varepsilon_x\right)\sin\theta\cos\theta + \left(2\varepsilon_{45} - \varepsilon_x - \varepsilon_y\right)\left(\cos^2\theta - \sin^2\theta\right)} \tag{12}$$

$$S = P_{t,u}\sin\theta\cos\theta / A \tag{13}$$

where, P_t is load; ε_x, ε_y, ε_{45} are the strain obtained from strain gauges in Fig.2; $P_{t,u}$ is the ultimate load; A is the sectional area of the middle part of the specimen.

Shear strength of LBL obtained by Eq.(13) is shown in Fig.10(a). As one can see, the calculated shear strength decreases almost linearly with the increase in alignment angle, which was because the mean tensile strength of 0° specimens was much greater than that of other specimens, leading to the smaller and smaller calculated values of shear strength. Thus, for better application of off-axis tension test on determining shear properties in engineering use, the shear strength calculated in this paper and the results obtained from off-axis compression test was compared (Yang et al. 2020) (shear strength=14.7MPa, COV=13.24%). It was

found that they did not agree with each other, so the test method recommended in ASTM D143 was applied to the shear strength of LBL (shear strength=14.2MPa, COV=10.90%, as shown in Fig.11), and the results are also shown in Fig.10(a). The shear strength obtained by off-axis compression test and ASTM method was very close. Considering that LBL is a bio-based material, so to speak, the result from off-axis compression test and ASTM method was nearly the same. To obtain shear strength of LBL for engineering use from tension test with different fiber alignment angles, a fitted empirical equation was proposed:

$$S^* = \frac{P_{t,u} \sin\theta\cos\theta}{A} + 0.18 \times \frac{\theta}{180^o} \times 180 - 1.5 \quad 15^o \le \theta \le 75^o \tag{14}$$

where, S^* is the revised shear strength.

As for shear modulus, it can be seen from Fig.10(b) that the mean values of the specimens with 15°, 30° and 60° were close, while the mean values of 45° and 75° specimens were lower. The mean value of shear modulus calculated in this paper was 1048.5MPa with COV of 24%, which was slightly lower than that of 1164.8MPa obtained from off-axis compression test. Itt may be because LBL was more solid under compression, so the value of shear modulus increased. However, since off-axis test was not recommended for calculating shear modulus in standards, more test methods need to be studied and compared.

All the shear properties of the five groups are shown in Table 2.

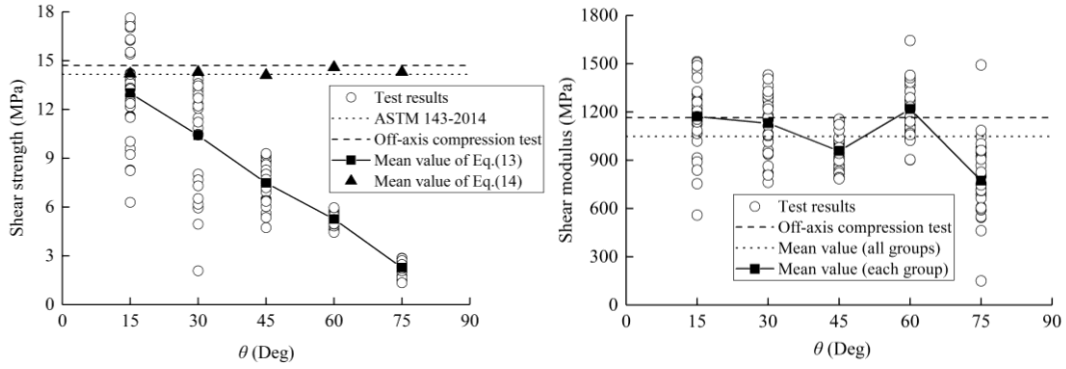

(a) Shear strength (b) Shear modulus

Fig.10 Shear properties

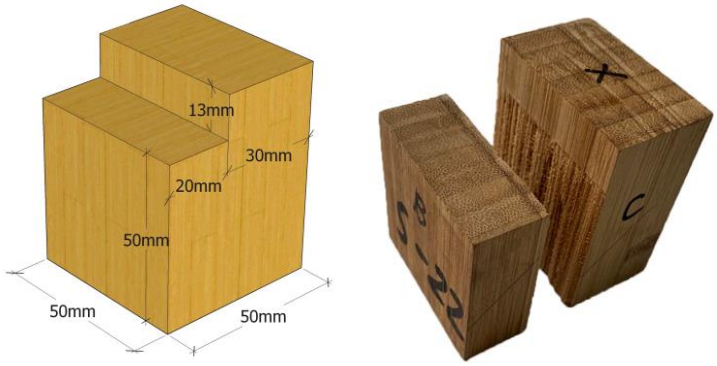

(a) sample dimensions (b) sample after test

Fig.11 Shear test of ASTM 143

Table 2 Shear properties of LBL

Group		T15	T30	T45	T60	T75
Shear modulus /MPa	Mean	1171	1129	957	1219	772.2
	COV	0.189	0.163	0.116	0.140	0.233
Shear strength /MPa Eq.(13)	Mean	13.0	10.4	7.5	5.3	2.3
	COV	0.219	0.308	0.156	0.081	0.165
Revised shear strength /MPa Eq.(14)	Mean	14.2	14.3	14.1	14.6	14.3

6 Conclusion

In this paper, tensions tests on 210 specimens with fiber alignment angles from 0° to 90° were conducted to study the off-axis tensile properties of LBL. The results showed that the overall tensile failure type of LBL was brittle failure. With the increase in the alignment angle, the ultimate tensile strength, tensile modulus, and ultimate strain of the LBL decreased rapidly from 0° to 30°, while they almost remained constants after 45°. The Poisson's ratio increased at 0° to 15° and then decreased gradually. Hankinson's formula (n=1.75) can be used to predict the tensile strength of LBL. An empirical equation was proposed to predict the tensile modulus of LBL.

Based on the stress-strain coordinate transformation, the relation between shear properties and the alignment angle of LBL was studied. The calculated shear strength decreased with increasing alignment

angle, which was far less from the shear strength calculated by ASTM D143, and off-axis compression test. Thus, an empirical equation was proposed which could be used to obtain the shear strength of LBL for engineering use by off-axis tension test. While the shear modulus obtained from off-axis tensile test in this paper was slightly smaller than that of off-axis compression test, it may be due to the compression test making the material more compact, which needs further research.

Funding: This work was supported by the National Natural Science Foundation of China (No. 51878354 & 51308301); the Natural Science Foundation of Jiangsu Province (No. BK20181402 & BK20130978); Postgraduate Research &Practice Innovation Program of Jiangsu Province (KYCX21_0902); Six talent peak high-level projects of Jiang-su Province (No. JZ-029); and a Project Funded by the Priority Academic Program Development of Jiangsu Higher Education Institutions. Any research results expressed in this paper are those of the writer(s) and do not necessarily reflect the views of the foundations.

Acknowledgment: The writers gratefully acknowledge Chaokun Hong, Han Zhang, Ke Zhou, Zhen Wang, Hang Li, Xiaoyan Zheng, Shaoyun Zhu, Liqing Liu, Dunben Sun, Jing Cao, Yanjun Liu and others from the Nanjing Forestry University for helping.

The authors declare that they have no conflicts of interest to this work.

References

Allwood J M, Cullen J M, Carruth M A, et al. (2012) Sustainable materials: with both eyes open. Cambridge, UK: UIT Cambridge Limited.

ASTM International (2014) Standard test methods for small clear specimens of timber ASTM D143-2014. US, ASTM International.

Bi W, Li H, Hui D, Gaff M, Lorenzo R, Corbi I, Corbi O, Ashraf M (2021) Effects of chemical modification and nanotechnology on wood properties. Nanotechnol Rev 10(1): 978-1008. https://doi.org/10.1515/ntrev-2021-006

Bodig J, Jayne B A (1982) Mechanics of wood and wood composites. New York: Van Nostrand Reinhold.

Chen G, Jiang H, Yu Y, Zhou T, Wu J, Li X (2020) Experimental analysis of nailed LBL-to-LBL connections loaded parallel to grain. Mater Struct 53(4):1-13. https://doi.org/10.1617/s11527-020-01517-5

British Standard (2002). EN 1990 Eurocode: Basis of structural design. United Kingdom: British Standards Institute.

Chen L F, Su H T, Liu L, Zhang Y J, Wang Y X (2007) Experimental study on corrosion resistance and natural corrosion resistance of 11 kinds of bamboo. Guangdong For Sci Technol 23(1):34-36. http://www.gdforestscience.com/ch/reader/download_pdf.aspx?file_no=20070115&year_id=2007&quarter_id=1&falg=1

Chow A, Ramage M H, Shah D U (2019) Optimising ply orientation in structural laminated bamboo. Constr Build Mater 212:541-548. https://doi.org/10.1016/j.conbuildmat.2019.04.025

Corbi O, Baratta A, Corbi I, Tropeano F (2021) Design issues for smart seismic isolation of structures: past and recent research. Sustain Struct 1(1): 000001. https://doi.org/10.54113/j.sust.2021.000001.

Correal J F, Echeverry J S, Ramírez F, Yamín L E (2014) Experimental evaluation of physical and mechanical properties of Glued Laminated Guadua angustifolia Kunth. Constr Build Mater 73:105-112. https://doi.org/10.1016/j.conbuildmat.2014.09.056

Dauletbek A, Li H, Xiong Z, Lorenzo R (2021) A review of mechanical behavior of structural laminated

bamboo lumber. Sustain Struct 1(1): 000004. https://doi.org/10.54113/j.sust.2021.000004

Díaz G A, Cruz R A, Chávez A M (2013) Optimization of the bamboo guadua angustifolia kunth in the elaboration of glued laminated elements for constructive use. In: Journal of Physics: Conference Series. IOP Publishing Vol.466, No.1, p.012032. https://iopscience.iop.org/article/10.1088/1742-6596/466/1/012032/meta

Ghavami K (2008) Modern bamboo structures. CRC Press p.17-34.

Hankinson R L (1921) Investigation of crushing strength of spruce at varying angles of grain. Air service information circular 3(259):130.

Huang D, Bian Y, Zhou A, Sheng B (2015) Experimental study on stress–strain relationships and failure mechanisms of parallel strand bamboo made from phyllostachys. Constr Build Mater 77:130-138. https://doi.org/10.1016/j.conbuildmat.2014.12.012

Khoshbakht N, Clouston P L, Arwade S R, Schreyer A C (2018) Computational modeling of laminated veneer bamboo dowel connections. J Mater Civil Eng 30(2):04017285. https://doi.org/10.1061/(ASCE)MT.1943-5533.0002135

Lee C H, Chung M J, Lin C H, Yang T H (2012) Effects of layered structure on the physical and mechanical properties of laminated moso bamboo (Phyllosachys edulis) flooring. Constr Build Mater 28(1):31-35. https://doi.org/10.1016/j.conbuildmat.2011.08.038

Lei W, Zhang Y, Yu W, et al. (2021) The adsorption and desorption characteristics of moso bamboo induced by heat treatment. J For Eng 2021, 6(3): 41-46. http://lygcxb.njfu.edu.cn/#/digest?ArticleID=4504

Leng Y, Xu Q, Harries K A, Chen L, Liu K, Chen X (2020) Experimental study on mechanical properties

of laminated bamboo beam-to-column connections. Eng Struct 210:110305. https://doi.org/10.1016/j.engstruct.2020.110305

Li H, Wang B J, Wang L, Wei P, Wei Y, Wang P (2021). Characterizing engineering performance of bamboo-wood composite cross-laminated timber made from bamboo mat-curtain panel and hem-fir lumber. Compos Struct 266: 113785. https://doi.org/10.1016/j.compstruct.2021.113785

Li H T, Su J W, Zhang Q S, Chen G (2015a) Experimental study on mechanical performance of side pressure laminated bamboo beam. J Build Struct 36(3):121-126. https://en.cnki.com.cn/Article_en/CJFDTotal-JZJB201503016.htm

Li H T, Su J W, Zhang Q S, Deeks A J, Hui D (2015b) Mechanical performance of laminated bamboo column under axial compression. Compos Part B-Eng 79:374-382. https://doi.org/10.1016/j.compositesb.2015.04.027

Li H T, Zhang Q S, Huang D S, Deeks A J (2013) Compressive performance of laminated bamboo. Compos Part B-Eng 54:319-328. https://doi.org/10.1016/j.compositesb.2013.05.035

Li Y J, Lou Z C (2021) Progress of bamboo flatten technology research. J For Eng 2021, 6(4): 14-23. http://lygcxb.njfu.edu.cn/#/digest?ArticleID=4527

Liu H, Yang X, Zhang X, Su Q, Zhang F, Fei B (2021) The tensile shear bonding property of flattened bamboo sheet J For Eng 2021,6(01):68-72. http://lygcxb.njfu.edu.cn/#/digest?ArticleID=4452

Liu J, Zhou A, Sheng B, et al. (2020a) Effect of temperature on short-term compression creep property of bamboo scrimber. J For Eng 6(2): 64-69. http://lygcxb.njfu.edu.cn/#/digest?ArticleID=4478

Liu W, Hu X, Yuan B, Xu F, Huang J (2020b) Tensile strength model of bamboo srimber by 3-pb fracture test on the basis of non-LEFM. Compos Sci Technol 108295.

https://doi.org/10.1016/j.compscitech.2020.108295

Lorenzo R, Godina M, Mimendi L, Li H T (2020a) Determination of the physical and mechanical properties of moso, guadua and oldhamii bamboo assisted by robotic fabrication. J Wood Sci 66(1):1-11. https://doi.org/10.1186/s10086-020-01869-0

Lorenzo R, Mimendi L, Godina M, Li H T (2020b) Digital analysis of the geometric variability of Guadua, Moso and Oldhamii bamboo. Constr Build Mater 236:117535. https://doi.org/10.1016/j.conbuildmat.2019.117535

Lou Z, Wang Q, Sun W, Zhao Y, Wang X, Liu X, Li Y (2021). Bamboo flattening technique: a literature and patent review. Eur J Wood Wood Prod 1-14. https://doi.org/10.1007/s00107-021-01722-1

Mahdavi M, Clouston P L, Arwade S R (2011) Development of laminated bamboo lumber: review of processing, performance, and economical considerations. J Mater Civil Eng 23(7):1036-1042. https://doi.org/10.1061/(ASCE)MT.1943-5533.0000253

National Standards of China (2003). Code for Design of Timber Structures (GB 50005) Architecture and Building Press, Beijing.

Pindera M J, Herakovich C T (1986) Shear characterization of unidirectional composites with the off-axis tension test. Exp Mec 26(1):103-112.

Ponzo FC, Antonio DC, Nicla L, Nigro D (2021) Experimental estimation of energy dissipated by multistorey post-tensioned timber framed buildings with anti-seismic dissipative devices. Sustain Struct 1(2): 000007. https://doi.org/10.54113/j.sust.2021.000007.

Sharma B, Bauer H, Schickhofer G, Ramage M H (2017) Mechanical characterisation of structural laminated bamboo. P I Civil Eng-Str B 170(4):250-264. https://doi.org/10.1680/jstbu.16.00061

Sinha A, Way D, Mlasko S (2014) Structural performance of glued laminated bamboo beams. J Struct Eng 140(1):04013021. https://doi.org/10.1061/(ASCE)ST.1943-541X.0000807

Su J, Li H, Xiong Z, Lorenzo R (2021) Structural design and construction of an office building with laminated bamboo lumber. Sustain Struct 1(2): 000010. https://doi.org/10.54113/j.sust.2021.000010

Sun F L, Prosper N K, Wu H P, Qian J J, Yang X S, Rao J, Guo M (2017) A review on the development of wood and bamboo preservation. J For Eng 2:1-8. http://lygcxb.njfu.edu.cn/#/digest?ArticleID=3911

Takeuchi C P, Estrada M, Linero D L (2016) The Elastic Modulus and Poisson's Ratio of Laminated Bamboo Guadua angustifolia. In: Key Engineering Materials. Trans Tech Publications Ltd Vol.668, p.126-133. https://doi.org/10.4028/www.scientific.net/KEM.668.126

Verma C S, Chariar V M (2013) Stiffness and strength analysis of four layered laminate bamboo composite at macroscopic scale. Compos Part B-Eng 45(1):369-376. https://doi.org/10.1016/j.compositesb.2012.07.048

Wei Y, Zhao K, Hang C (2020) Stress–strain relationship model of glulam bamboo under axial loading. Adv Compos Lett 29:2633366X20958726. https://doi.org/10.1177/2633366X20958726

Wu K T (1992) The effect of high-temperature drying on the antisplitting properties of makino bamboo culm (Phyllostachys makinoi Hay.) Wood Sci Technol 26(4):271-277. https://doi.org/10.1007/BF00200162

Xiao F, Wu Y, Zuo Y, Peng L, Li W, Sun X (2021) Preparation and bonding performance evaluation of bamboo veneer/foam aluminum composites J For Eng 2021,6(03):35-40. http://lygcxb.njfu.edu.cn/#/digest?ArticleID=4503

Xiao Y, Yang R Z, Shan B (2013) Production, environmental impact and mechanical properties of

glubam. Constr Build Mater 44: 765-773. https://doi.org/10.1016/j.conbuildmat.2013.03.087

Xu Q, Leng Y, Chen X, Harries K A, Chen L, Wang Z (2018) Experimental study on flexural performance of glued-laminated-timber-bamboo beams. Mater Struct 51(1): 9. https://doi.org/10.1617/s11527-017-1135-2

Yang D, Li H, Xiong Z, Mimendi L, Lorenzo R, Corbi I, Corbi O, Hong C (2020) Mechanical properties of laminated bamboo under off-axis compression. Compos Part A-Appl Sci Manuf 138:106042. https://doi.org/10.1016/j.compositesa.2020.106042

Yuan T, Han X, Wu Y, Hu S, Wang X, Li Y (2021). A new approach for fabricating crack-free, flattened bamboo board and the study of its macro-/micro-properties. Eur J Wood Prod 79(6): 1531-1540. https://doi.org/10.1007/s00107-021-01734-x

Zhong Y, Wu G, Ren H, Jiang Z (2017) Bending properties evaluation of newly designed reinforced bamboo scrimber composite beams. Constr Build Mater 143:61-70. https://doi.org/10.1016/j.conbuildmat.2017.03.052

Zhou Y, Huang Y, Sayed U, Wang Z (2021) Research on dynamic characteristics test of wooden floor structure for gymnasium. Sustain Struct 1(1): 000005. https://doi.org/10.54113/j.sust.2021.000005